J. Applied Membrane Science & Technology, Vol. 28, No. 1, April 2024, 27–46

Investigating Hydrocarbon Gases Permeability Through Hollow Fiber Hybrid Carbon Membrane

A. R. Widyanto[a,b], I. S. Caralin[a,b,c], Nurul Widiastuti[a]*, Triyanda Gunawan[a], Rika Wijiyanti[a,d], A. F. Ismail[e], W. N. W. Salleh[e], Mikihiro Nomura[b], Kohei Suzuki[b]

[a]Department of Chemistry, Faculty of Science and Data Analytics, Institut Teknologi Sepuluh Nopember, Sukolilo, Surabaya 60111, Indonesia
[b]Department of Applied Chemistry, Shibaura Institute of Technology, 3-7-5 Toyosu, Koto-ku, Tokyo 135-8548, Japan
[c]Regional Environment Systems, Shibaura Institute of Technology, 3-7-5 Toyosu, Koto-ku, Tokyo 135-8548, Japan
[d]Medical Intelligence Postgraduate Program, Sekolah Tinggi Intelijen Negara (State Intelligence College), Sumur Batu, Babakan Madang, Bogor, 16810, Indonesia
[e]Advanced Membrane Technology Research Center (AMTEC), Universiti Teknologi Malaysia, 81310 UTM Johor Bahru, Johor, Malaysia

Submitted: 3/11/2023. Revised edition: 29/2/2024. Accepted: 29/2/2024. Available online: 28/3/2024

ABSTRACT

Hydrocarbon separation from natural gases is a critical procedure in the chemical and petrochemical industries. This study used hollow fiber carbon membranes (HFCMs) made from a commercially available co-polyimide, P84, with zeolite-carbon composite (ZCC) as a filler to separate light hydrocarbons like CH_4/C_3H_8 and CH_4/C_2H_6. The Arrhenius technique was used to evaluate the effects of temperature fluctuations (298, 323, and 373 K) on the membrane. X-ray diffraction exhibited a characteristic graphite peak at $2\theta \sim 44°$, indicating the creation of an effective carbon membrane. SEM investigation revealed the compactness of both pristine and hybrid carbon membrane structures. The operating temperature has a significant influence on the gas penetration through the membrane when evaluating gas permeation. The hybrid carbon membrane has the highest permeability for CH_4, C_2H_6, and C_3H_8 at 373 K. (81.86, 61.82, and 58.28 Barrer, respectively). The carbon membrane also showed greatest selectivity for CH_4/C_3H_8 and CH_4/C_2H_6 at 323 K (2.24 and 2.04, respectively). Adsorption and surface diffusion were the membrane's transport mechanisms. By adding filler to the membrane, the gas permeability was temperature dependent.

Keywords: Carbon membranes, carbon, gas separation, thermodynamic properties, hydrocarbon, permeability

1.0 INTRODUCTION

Natural gas is a significant source of energy and is frequently used as a fuel in thermal units in a variety of power systems. Global natural gas consumption is predicted to exceed 110 trillion standard cubic feet per year and is expected to surpass 200 trillion standard cubic feet per year by 2040 [1], [2]. Natural gas is composed mostly of methane (CH_4), ethane (C_2H_6), and propane (C_3H_8) [3]. Separating hydrocarbons from raw gases is a vital step in the production of chemicals [4]. Various techniques exist for the separation of hydrocarbons at the moment. These include adsorption and rectification procedures, as well as cryogenic and

* Corresponding to: Nurul Widiastuti (email: nurul_widiastuti@chem.its.ac.id)
DOI: https://doi.org/10.11113/amst.v28n1.284

membrane technology. Membrane technology has a number of benefits over more conventional techniques. It is distinguished by high energy efficiency, reliability, simplicity of operation, cheap cost, and environmental friendliness [5]. Membranes for gas separation are classed according to their material, as polymeric or inorganic. Interestingly, as compared to polymeric membranes, inorganic membranes are substantially more resistant to the plasticizing impact of these condensable gases [4,6]. Inorganic membrane materials including zeolite, silica, metal oxide, and carbon are used [7–14]. Carbon membranes provide a variety of advantages, including simplicity of manufacture, variable porosity, and excellent chemical and thermal stability. Furthermore, carbon membranes are useful for practically all gas separation applications [15].

The polymer precursor used in the fabrication of a carbon membrane has an effect on its gas permeation properties [16]. Glassy polymers are advantageous as precursors due to their low free volume and ultra-micropore structure [17]. Polysulfone membrane [18–23], and polyimide [24–29] have been investigated in the previous studies. On the other hand, carbon-based polyimide was favored in this work owing to its ability to preserve its structure after carbonization as it has a higher glass transition temperature than polysulfone [30–32]. Moreover, employing zeolite composite carbon (ZCC) as a filler in a P84 polymeric membrane could enhance CO_2 permeability (from 0.67 to 12.67 Barrer) and CO_2/CH_4 selectivity (from 0.76 to 2.10) [28]. ZCC, which was a previous product during ZTC synthesis. In addition, due to the kinetic diameter of light hydrocarbons, which ranges between 3.75 and 5.12 Å, porous structures with consistent microporosity are desirable. Due to its uniform pore structure, high micropore area, and compatible with carbon membrane filler particles, ZCC potentially applied as a filler for carbon membranes to separate light hydrocarbon, which has kinetic diameter of 3.75-5.12 Å [31,33]. Thus, the significance of ZCC filler in carbon membrane-based polyimide for hydrocarbon separation is investigated in this research (CH_4, C_3H_8 and C_2H_6). On the other hand, studying operation temperature exhibited separation behavior of gas permeability in membrane. As reported by Stevens *et al*. [34], gases permeability improved at higher temperature operation while permeation activation energies enhanced by higher gas kinetic dimensions. H_2 and CO_2 permeability, and its selectivity enhanced by higher temperature (from 35 to 190 °C), from 3.7, 0.29 Barrer and 12.75 to 31, 1.7 Barrer and 18, respectively, with H_2 and CO_2 activation energies was 16 and 13.3 kJ mol^{-1} [34]. Furthermore, the temperature dependency of the gas permeation was attributed to the existence of diffusion and sorption coefficients. The diffusion coefficient rise by higher temperature since the positive diffusion activation energies, but the sorption coefficient declines because of typical negative heats of sorption [35]. However, there is a lack of temperature dependence of hydrocarbon gases on carbon membrane report. Therefore, the objectives of this work are to better understand the permeability characteristics of carbon membrane at elevating temperature. The hydrocarbon gases (i.e., CH_4, C_3H_8, and C_2H_6) permeated on P84 pristine carbon membrane (CM) and a P84/ZCC hybrid carbon membrane (HCM) were investigated at different temperatures (298, 323, and 373K). Thermodynamic and activation energy

analyses were performed to evaluate the permeability and adsorption characteristics of the carbon membrane used in this study.

2.0 METHODS

2.1 Materials

A P84 pristine membrane, a P84/ZCC membrane, and ultrahigh purified N_2 gas were used to produce the carbon membrane. The gas permeability experiments were conducted using an epoxy resin, a P84 pristine carbon membrane, P84/ZCC hybrid carbon membrane and ultrapure CH_4, C_2H_6, and C_3H_8 gases (99.99 percent purity).

2.2 Preparation of Carbon Membranes

Gunawan *et al*. [28] previously described a technique for the fabrication of the P84 pristine membrane and the P84/ZCC mixed matrix membrane. Thereafter, using a N_2 carbonization method, all membranes were carbonized. Before carbonization at high temperature required one hour stabilizing at 300 °C at 3 °C/min rate. The temperature was then raised up to 700 °C during a one-hour period at the same heating rate. Finally, allowed the heat to drop to ambient temperature gradually.

2.3 Carbon Membranes Characterization

The d-spacing shift during the forming carbon membrane's structure was analyzed using X-ray diffraction (XRD-Philips PW1140/90). The membrane's morphology was examined by field emission scanning electron microscope (FESEM, JSM-7610F, JEOL) set to 15 kV. The membrane's pore characteristics were determined by N_2 isotherm adsorption desorption (Micromeritics, ASAP 2020). Thermal gravimetric analysis (TGA) was utilized to investigate the thermal stability of all carbon membranes. The TGA test parameter included heating the membrane continuously in a N_2 or air atmosphere (50 mL/min) at temperatures ranging from 25 to 800 °C at a rate of 10 °C/min.

2.4 Gases Permeability Evaluation

Methane, ethane, and propane were used in the pure gas permeability studies. Gas permeabilities were determined at various working temperatures, namely 298, 323, and 373 K. Figure 1 depicts the gas permeability test setup.

2.5 Analysis of Thermodynamic Approach

Thermodynamic analysis was used to characterize the permeation properties of CH_4, C_2H_6, and C_3H_8 molecules passing through a carbon membrane. The following equation (Equation (1)) was used to calculate the thermodynamic parameters:

$$ln\frac{p}{p_0} = \frac{\Delta H}{RT} - \frac{\Delta S}{R} \qquad (1)$$

in which ΔH exhibited the permeability enthalpy (kJ mol^{-1}), T indicated the Kelvin temperatures, p denoted the pressure of equilibrium state (bar), and R was molar gas constant (8.314 J mol^{-1} K^{-1}) [31].

2.6 Analysis of activation energy approach

The activation energy was determined utilizing Arrhenius formula (Equation (2)) as shown in:

$$\ln P = -\frac{E_a}{RT} + lnP_0 \qquad (2)$$

In which E_a represented as energy of activation (kJ mol^{-1}), T denoted the Kelvin temperatures, P symbolized the gas permeabilities (mol m^{-1} s^{-1} Pa^{-1}), A represented the pre-exponential variable, and R was the gas constant (8.314 J mol^{-1} K^{-1}) [36].

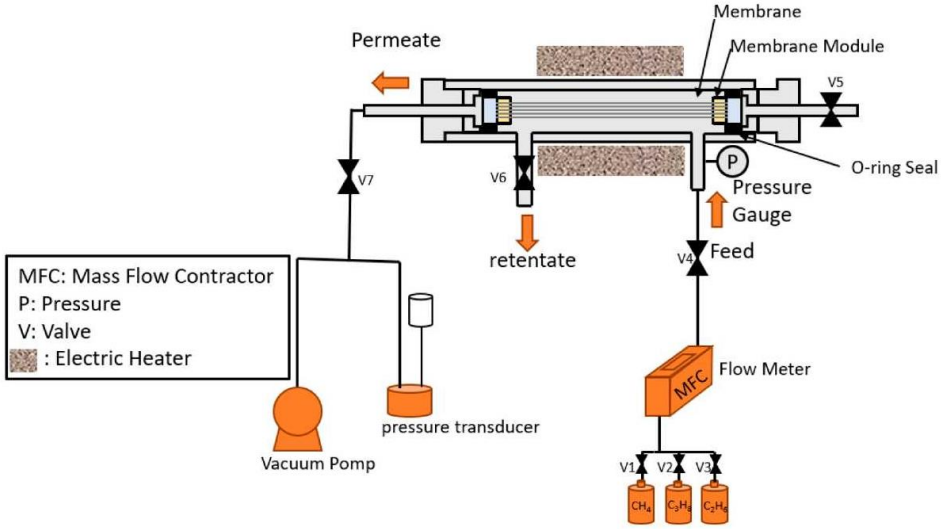

Figure 1 An illustration of gas permeability test setup

3.0 RESULTS AND DISCUSSION

3.1 Preparation of the CM and HCM

The carbon membrane was modified in this work by adding ZCC filler. The XRD analysis revealed a change in the microstructure phases and d-spacing number of the carbon membrane because of the ZCC existence, as seen in Figure 2. The d-spacing number demonstrated that the length within the layers of the carbon membrane served as a channel for gas diffusion across the membrane [37, 38]. Moreover, this study was continuity of the previous research, we have successful synthesis ZCC and utilized it as a filler in P84 polymeric membrane and the discussion of XRD characterizations of ZCC has been reported by Gunawan *et al*. [28], which ZCC exhibit similar typical patterns of Zeolite Y at 2θ of 6, 10, 11.8, 15.5, 18.6, 20.2, 23.5, 26.9, 29.4, 30.5, 31.2, 32.3, 33.9, 34.5, 37.6, and 41.1 [39, 40].

All carbon membranes had amorphous structures (002) and aromatic graphite (100) at 2 around 22º and 42-44º, respectively [41]. The graphite peak [100] was observed, indicating the carbon production in the membrane [42]. At the highest peaks, the largest numbers for d-spacing were attained. These were the mean distances within the chain segments' centers in the copolymer [43]. The polymeric P84 pristine membrane's d-spacing number was discovered to be 4.98 (Å). Upon carbonization, a drop in the d-spacing values to 3.93 and 3.94 (Å) was observed, indicating the development of the carbon membrane. The results indicated that a more compact structure with a greater packing density were formed as well as the production of a microstructure with densely packed graphite layers from a polymeric precursor [44]. The obtained structure has decreased diffusion gaps for small gas molecules passing across the P84 pristine carbon membrane [45]. The hybrid carbon membrane has a greater peak intensity than the carbon

membrane since it is loaded with ZCC that has uniform structure. However, by adding filler to the carbon membrane, a larger d-spacing number in the aromatic graphite phase [100] was observed. Following that, the graphitic structures realignment lead to a change in the pore size distribution favor larger micropores [46].

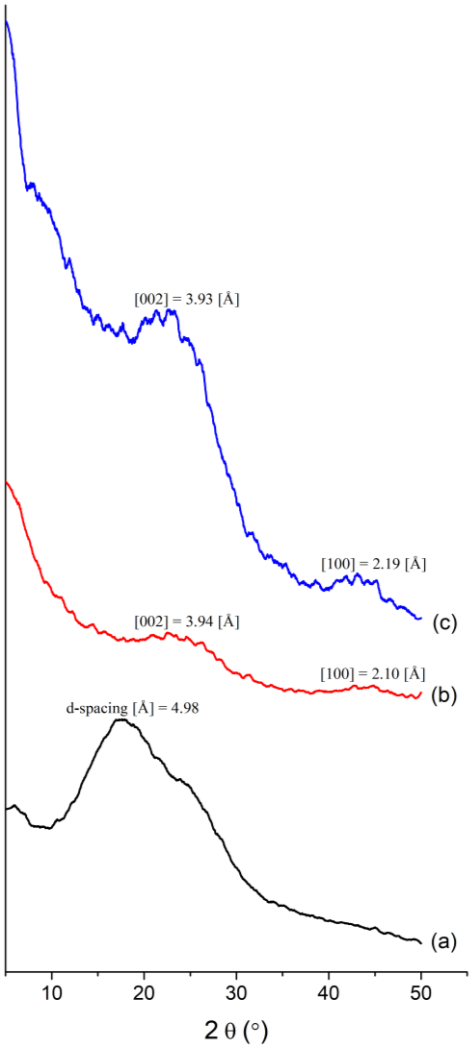

Figure 2 XRD pattern of (a) the P84 membrane, (b) carbon membrane, and (c) hybrid carbon membranes (Adopted from [31])

The XRD discussion was supported with the SEM examination, which was utilized to investigate the cross-sectional morphology of the pristine carbon membrane and hybrid carbon membrane. Carbonization of the P84 pristine membrane and the P84/ZCC mixed matrix membrane was found to be effective, as shown by the compact and dense membrane structures (Figure 3).

TGA was used to determine the thermal stability of pure carbon and hybrid carbon membranes, as seen in Figure 4. All carbon membranes lose mass at temperatures below 100 °C due to the evaporation of adsorbed water [24]. The carbon membrane and its hybrid exhibit exceptional heat stability up to 800 °C with a mass loss of 15-16%. Carbonization of their mixed matrix membrane (P84/ZCC) enables a considerable increase in membrane thermal stability [47]. Although a significant difference in mass loss between the carbon hybrid membrane and its pristine membrane was observed below 500 °C, which was attributed to the presence of a zeolite framework with a tendency to adsorbed moisture, it was demonstrated that the presence of ZCC improves thermal stability by slowing the membrane's decomposition rate between 500 and 540 °C. At 602.37 and 591.5 °C, respectively, the carbon membrane and its composite displayed the fastest breakdown rates, with a residual mass of 3.19 and 2.25%.

Porous inorganic membrane gas separation performance was dependent on the pore structure. A small pore diameter, i.e., 0.6 nm (ultra-micropore) or 0.6–2 nm (micropore), was typically preferred for porous inorganic membranes such as carbon ones. The range of the membrane pore diameter was deemed suitable based on the gas kinetic diameter (< 0.4 nm). Thus, membranes are able to separate gases via a molecular sieving mechanism [15, 48]. On another hand, porous inorganic membranes with range pores of 0.5-2 nm controlled by a mechanism diffusion within molecular sieving,

Knudsen diffusion, and/or surface diffusion [49]. The conducted pore structure analysis enabled characterization of the carbon membrane using a N_2 adsorption isotherm. The investigation of the pore size distribution (PSD) was performed using the SAIEUS program and the 2D-NLDFT theory [40].

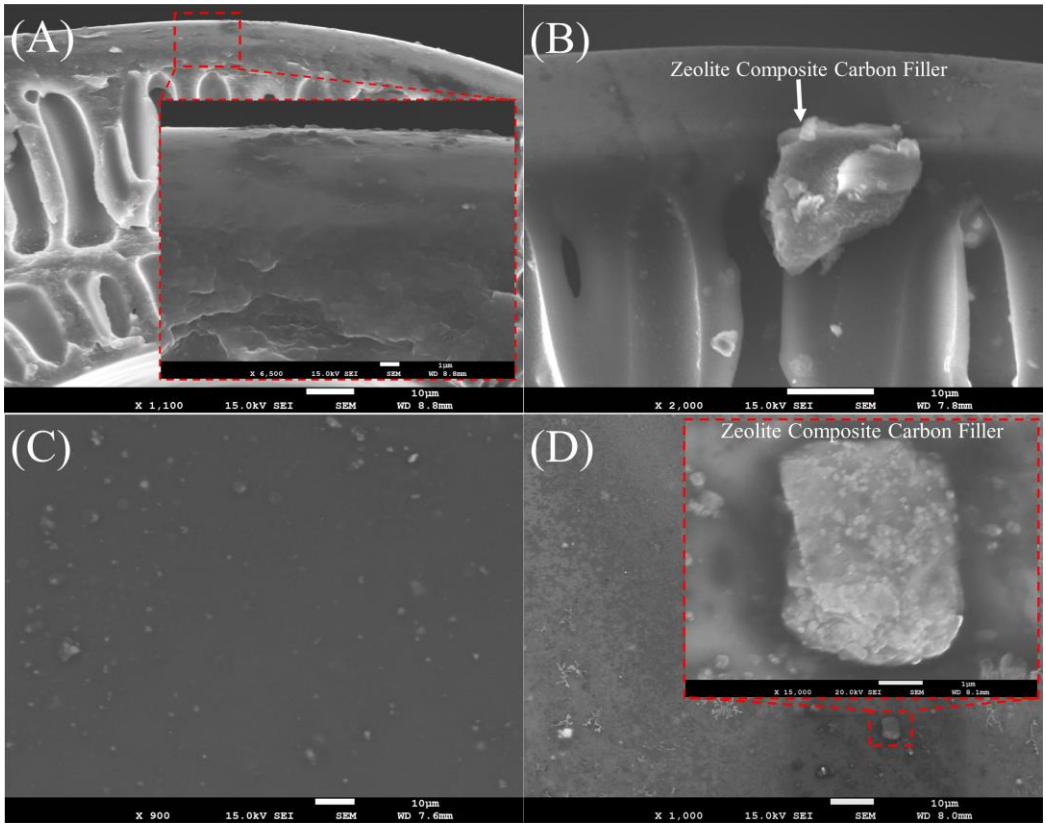

Figure 3 SEM image cross section and surface of (a,c) P84 carbon membrane and (b,d) hybrid carbon membrane

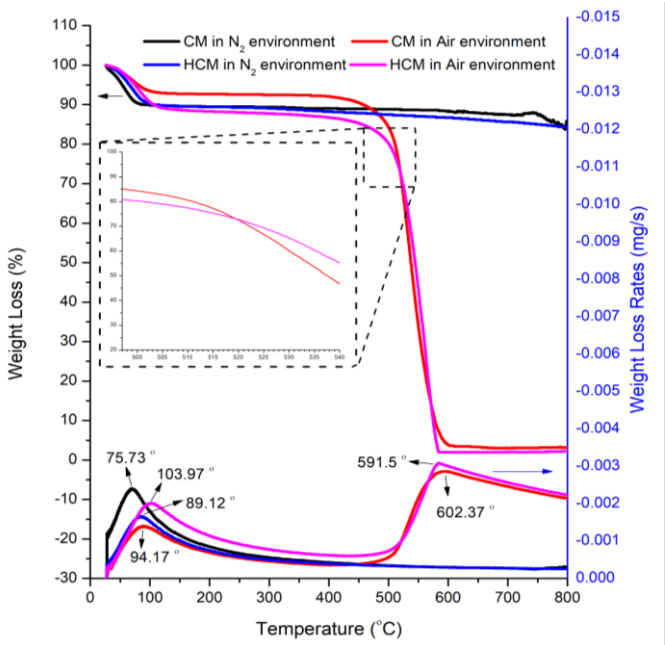

Figure 4 TGA analysis of P84 carbon membrane (CM) and hybrid carbon membrane (HCM)

Figure 5 displayed the N_2 adsorption properties of each membrane, while Table 1 summarized the measured values. As expected, the carbon membrane produced a type I adsorption isotherm compatible with the IUPAC categorization. This indicated that HFCMs were composed entirely of carbon matrix and micropores. Whereas hybrid carbon membranes exhibited a kind IV adsorption isotherm in accordance with the IUPAC, this was exhibited by the fact that the pore was not completely filled at low pressure due to adsorption appearing in the mesoporous via multilayer adsorption accompanied with pore condensation [50]. In comparison to published findings for a predecessor [51], the carbon membrane displayed greater S_{bet} and total pore volume. During pyrolysis, the volatile groups in the precursor were released and the atoms were rearranged. Volatile compounds were released, creating a new pore system, along with the membrane matrix. Hence, the surface area was improved due to the increasing degree of microporosity. If compared with the hybrid carbon membrane, The S_{bet} and S_{mic} value are lower due to the ZCC filler presence on the hybrid carbon membrane that can contribute to the surface area. The PSD of porous inorganic membranes is an important factor, which determines their gas transport mechanism. When the pore widths are 2–50 nm (mesopore), 2 nm (micropore), or 0.6 nm (ultra-micropore), membranes are known to follow Knudsen diffusion, surface adsorption, and molecular sieving, respectively [15]. Hence, determining the PSD of carbon membranes is important, as the gas transport and membrane performance can be predicted based on this value. The membrane was discovered to have a modest average hole size after being pyrolyzed at 700 °C. Accordingly, it was assumed that the membrane would display enhanced selectivity compared to the hybrid carbon membrane. The predominant mechanism of diffusion of the carbon membrane is molecular sieving. The different diffusion mechanisms showed on hybrid carbon membranes which a dominant combination both surface diffusion and Knudsen diffusion due to the existence of mesopore.

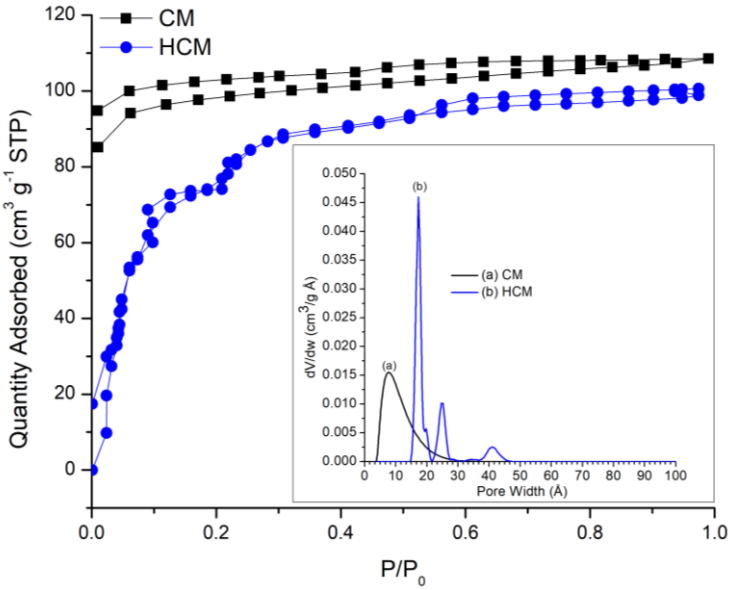

Figure 5 N_2 isotherm of the carbon membrane and hybrid carbon membrane pyrolyzed at 700 °C. Inset image shows the 2D-NLDFT pore distribution of the membrane

Table 1 Surface parameters of the P84 carbon membrane and hybrid carbon membrane

Sample	Pyrolysis (°C)	S_{bet} (m^2/g)	S_{mic} (m^2/g)	V_{tot} (cc/g)	Avg Pore Size (Å)
Precursor	-	20	-	0.094	19.0
Pristine Carbon Membrane	700	306.53	260.38	0.17	9.27
Hybrid Carbon Membrane [31]	700	373.04	268.09	0.15	17.29

3.2 Permeability Performance of the Carbon Membrane and Hybrid Carbon Membrane

The kinetic diameters of the gases (CH_4, C_2H_6, and C_3H_8) at ambient temperature impacted their separation on the carbon membrane and hybrid carbon membrane. As exhibited in Figure 6, CH_4 had a greater permeability than C_2H_6 and C_3H_8. C_3H_8 had a little greater permeability, nevertheless, the difference was not significant since the kinetic diameters of these gases were comparable. The gases permeability in the carbon membrane differed according to whether it was made using a polymer or MMM. Tirouni *et al*. [4] revealed that CH_4, C_2H_6, C_3H_8, and N_2 could be separated. The gas permeability was observed to decrease in the sequence $C_3H_8 > C_2H_6 > CH_4 > N_2$, indicating that it was regulated by the solution diffusion mechanism.

Gas diffusion was reliant on the pore size and kinetic diameter of the carbon membrane, since the carbon membrane's primary contribution was due to molecular sieving [52]. In comparison to the polymer membrane precursor, the carbon membrane displayed a small pore size, resulting in a more compact structure and a narrow pore size distribution. The presence of ZCC on the carbon membrane results in an increase in the membrane's pore diameters, from 0.93 - 1.73 nm. Thus, it is expected that the hybrid carbon membrane could have a greater permeability.

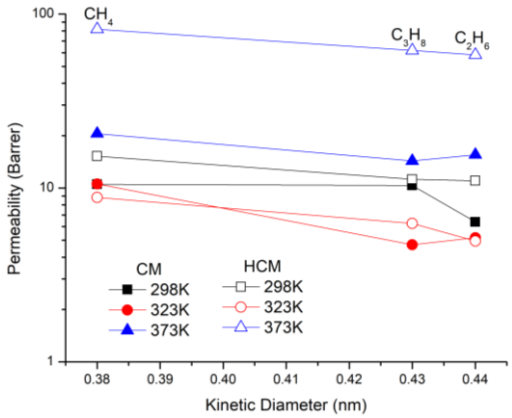

Figure 6 Permeability of CH_4, C_2H_6, and C_3H_8 based on kinetic diameters

As exhibited in Figure 7 (a and b), the CH_4/C_2H_6 and CH_4/C_3H_8 separation were investigated at different operating temperatures (298, 323, and 373 K). At ambient temperature (298 K), the permeability values of the carbon

membrane for CH_4, C_2H_6, and C_3H_8 were determined at 10.52, 6.38, and 10.35 Barrer. The CH_4/C_2H_6 (1.65) and CH_4/C_3H_8 (1.02) selectivity was also established. ZCC existence on carbon membrane indicates the increasing of gases permeability values of CH_4, C_2H_6, and C_3H_8, which were determined at 15.25 (45.01%), 11.23 (8.56 %), and 11.01 (72.62%) Barrer, respectively, due to the higher average pore size in hybrid carbon membrane. However, the CH_4/C_2H_6 (1.39) selectivity occurred decreasing. This result similar with reported by Wu *et al*. [53]. The addition of filler on carbon membrane increases the permeability but decreases the selectivity of the pair gases due to the present of mesopore in hybrid carbon membrane. CH_4/C_3H_8 (1.36) selectivity was increased because of the production of large degree graphitic carbons with a rather rigid structure surrounding ZCC particles.

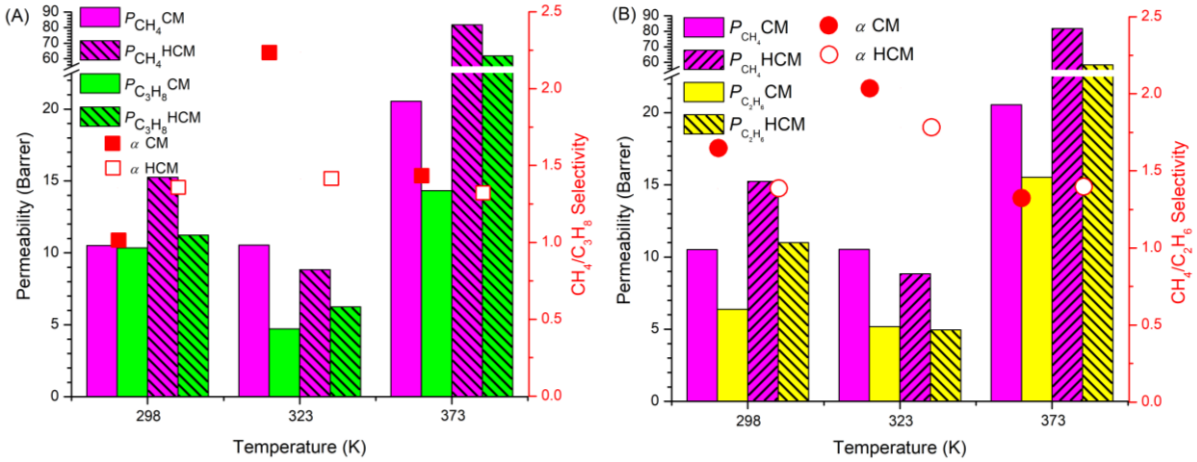

Figure 7 Permeability and selectivity of (a) CH_4/C_3H_8 and (b) CH_4/C_2H_6 in the CM and the HCM at determined different temperatures

The highest selectivity was achieved on carbon membrane at 323 K. For CH_4/C_2H_6, a 23.53% increase was noted, while for CH_4/C_3H_8, the selectivity increased by 119.99%. The higher selectivity results correlated with the pore size distribution data on both carbon and hybrid carbon membranes. This temperature trend was unique, as a concurrent decrease in permeability was observed. At higher operating temperature (i.e., 373 K), the permeability on carbon membrane of CH_4, C_2H_6, and C_3H_8 increased by 95.38%, 38.46%, and 143.54%, respectively. Moreover, the CH_4/C_3H_8 selectivity increased by 41.11%, while the CH_4/C_2H_6 selectivity decreased by −19.77%. The highest permeability was found in hybrid carbon membrane, the increasing permeability values of the gases for CH_4, C_2H_6, and C_3H_8 were determined at 678.33%, 497.47%, and 814.10%, due to the contribution of adsorption site of the ZCC with higher surface area. In addition, higher temperatures resulted in greater kinetic energy and increased molecular permeabilities, enabling gas particles to diffuse at more quickly, thus enhancing permeability [1].

This tendency paralleled the findings of Favvas *et al*. [54]. The researchers employed a co-polyimide-based carbon membrane in their work. The working temperature was altered (313, 333, and 373 K), and it was observed that the permeability reduced

as the temperature increased to 333 K. This finding in this study is also similar with previous findings for other microporous membranes, namely the MFI zeolite membrane [55–58]. Commonly, raising the temperature improves the permeance of the microporous membranes. Declining permeance was observed at a specific temperature. However, the permeance rose further at higher temperatures. Because of temperature dependence, two competitive mechanisms potentially occur in microporous membranes: adsorption and activated surface diffusion. Molecules hop among adsorption activated sites in micropore-dependent mass transfer. Thus, raising the temperature aids the process by enhancing diffusion. However, the quantity of adsorbed gases and occupancy degrees are reduced [54].

At 323 K, the occupancy decreased, leading to decreased permeance. Once the working temperature was raised to 373 K, the adsorption influence was diminished. It was well established that molecules contained within pores retain its gaseous state as well as diffuse through one location (activated sites) to another by passing an energy barrier [54]. Translational diffusion takes place as a result of the micropore structure. Additionally, it was discovered that the final calcination temperature had an effect on the carbon membrane's characteristics (Table 2). A previous study reported that carbonization of P84 co-polyimide at high final temperature of 900 °C resulted in a higher micropore diameter of approximately 0.4 nm (ultra-micropore) [54]. Higher carbonization temperatures typically produce denser structures, which decrease gas permeability. Moreover, the variation in the carbonization module led to different outcomes. The membrane performance was also compared to commercial membranes previously reported by Kagramanov *et al*. [59]. It was determined that the P84-derived carbon membrane evaluated in the present study exhibited a significantly improved permeation rate with comparable selectivity. Thus, the potential of this membrane further applications and scale-up has been demonstrated.

Table 2 Permeation performance during the separation of CH_4/C_3H_8 and CH_4/C_2H_6 in the membrane

Membrane	**Temperature (K)**	**Permeability (Barrer)**			**Selectivity**		**Reference**
		CH_4	**C_3H_8**	**C_2H_6**	**CH_4/C_3H_8**	**CH_4/C_2H_6**	
Carbon Membrane P84 (700 °C)	298	10.52 ± 1.01	10.35 ± 0.29	6.38 ± 0.73	1.02	1.65	This Work
	323	10.55 ± 1.25	4.72 ± 0.19	5.18 ± 0.05	2.24	2.04	
	373	20.55 ± 1.45	14.33 ± 0.66	15.53 ± 0.17	1.43	1.32	
Hybrid Carbon Membrane P84/ZCC (700 °C)	298	15.25 ± 4.17	11.23 ± 1.11	11.01 ± 1.03	1.36	1.39	
	323	8.84 ± 0.38	6.25 ± 0.58	4.95 ± 0.46	1.41	1.79	
	373	81.86 ± 3.77	61.82 ± 5.12	58.28 ± 5.23	1.32	1.40	

Membrane	Temperature (K)	Permeability (Barrer)	Selectivity	Reference	Membrane	Temperature (K)	Permeability (Barrer)
Polyurethane/ Silica MMM	RT	16.79	118	44.49	0.14	0.38	[60]
Polyurethane/ Zeolite 4A MMM	RT	30.4	45.6	35.2	0.66	0.85	[4]
Polyurethane/ ZSM-5 MMM	RT	22.7	63.4	37	0.36	0.61	
6F-DABA carbon molecular sieve	RT	69.44	-	51.01	-	1.36	[61]
6FDA/BPDA-DAM carbon molecular sieve	RT	3.05	0.59	2.65	5.17	1.15	[62]
Matrimid carbon molecular sieve	RT	0.32	0.02	-	16	-	[63]

3.3 Analysis of Thermodynamics and Activation Energy Approach

Thermodynamics and activation energy studies utilizing the Arrhenius equation were also used to analyze the gas permeabilities result. The parameters examined were heat of enthalpies (ΔH), entropies (ΔS), as well as the alteration for the Gibbs free energies (ΔG) as determined by Equation 1. Plot of ln(p/p) vs 1/T provided a gradient equal to ΔH and an interception corresponding to ΔS (Table 3). The adsorption heat (i.e., enthalpy) value defined the vigor of the interaction of both the adsorbent (i.e., the active surface site in the carbon membrane or hybrid carbon membrane) and the adsorbate (CH_4, C_2H_6, and C_3H_8) [40]. The ΔH values of CH_4, C_2H_6, and C_3H_8 were all negative (−0.75, −5.29, −5.44 kJ mol^{-1}, respectively) in the carbon membrane and (−20.60, −13.49, −15.87 kJ mol^{-1}, respectively) in the hybrid carbon membrane, indicating that these gases were adsorbing in an exothermic process in the carbon membrane. Notably, ΔH was below 80 kJ mol^{-1}, demonstrating that physical adsorption impacted the interaction of the adsorbates and adsorbents [64]. Specifically, the contact was not mediated by chemical bonds but rather by dipole-dipole interactions among the adsorbent surface (i.e., the membrane surface) and the adsorbate's atoms (i.e., the gas molecules). Due to the adsorbate's small volume on the surface, a powerful contact between the adsorbate and adsorbent was possible [40]. This was a reasonable answer for the low permeabilities result at 323 K since both adsorption and activated surface diffusion contributed to the gas transport mechanism. Thus, a large drop in the C_3H_8 permeabilities (−54.42%) in comparison to C_2H_6 (-18.84%) was caused by the higher ΔH value of C_3H_8 than C_2H_6. Therefore, the CH_4/C_3H_8 selectivity was higher than the CH_4/C_2H_6 selectivity in carbon

membrane. Additionally, a 0.26% increase in the permeability of CH_4 at 323 K was observed. The rise is believed to be due to low ΔH, which results in poor interactions among the CH_4 adsorbate and the carbon membrane's active surface site. The introduction of ZCC filler to the carbon membrane provided a higher ΔH value than pristine carbon membrane, exhibiting the adsorption effect on hybrid carbon membrane was stronger. Dependence on the operating temperature at 323 K shows different results compared with the carbon membrane. The decreasing permeability of CH_4 was caused by a high value of ΔH. Higher CH_4/C_2H_6 selectivity was found than CH_4/C_3H_8 selectivity, contribution from stronger adsorption effect on C_2H_6 than C_3H_8. As a result, a large decrease in the gas permeability of C_2H_6 (-55.01%) was occurred in comparison to C_2H_6 (-44.32%).

The ΔS values for CH_4, C_2H_6, and C_3H_8 of both carbon and its hybrid carbon membranes were determined at 0.20, 0.19, 0.19 kJ mol^{-1} and at 0.14, 0.16, 0.15 kJ mol^{-1}, respectively. The increased unpredictability at the gas/solid interface during permeation was indicated by the positive ΔS values [65]. This exhibited that CH_4, C_2H_6, and C_3H_8 gases have the mobility to diffuse in carbon membrane pores.

All gases had negative ΔG values for all gases were negative (Table 2), indicating the diffusion process in the membrane was spontaneous [40]. Improvements of operating temperature contributed to a rise for Gibbs free energy, suggesting that at greater operating temperature, gas adsorbed in membrane pores proceeded more spontaneously. Yet, the adsorption influence was ignored at 373 K. Additionally, it was interesting to note that the activation energy or the energy barrier had a greater effect on the permeability. Table 3 summarized the activation energy values determined using Equation (2). C_3H_8 (5.07 kJ mol^{-1}) had a smaller activation energy in a carbon membrane than CH_4 (8.37 kJ mol^{-1}) and C_2H_6 (11.99 kJ mol^{-1}). Importantly, it was determined that the activation energy took effect at 373 K. The sequence of decreasing permeability was $C_2H_6 > CH_4 > C_3H_8$. The activation energy was expected to operate as an energy barrier for active surface diffusion. It was also supposed that higher activation energy suggested more significant penetration into the micropores. Thus, the CH_4/C_3H_8 selectivity was higher than the CH_4/C_2H_6 selectivity. The inclusion of ZCC results in a larger energy activation in the hybrid carbon membrane than in the carbon membrane. Indicating that gas penetration was more temperature dependent than carbon membrane owing to the ZCC's greater activated surface areas.

Table 3 Thermodynamic parameters and activation energy for CH_4, C_2H_6, and C_3H_8 permeabilities across carbon and hybrid carbon membranes

Membrane	Gas	Temperature (K)	ΔH (kJ mol^{-1})	ΔS (kJ mol^{-1})	ΔG (kJ mol^{-1})	Ea (kJ mol^{-1})
Carbon Membrane	CH_4	298	−0.75	0.20	−60.47	8.73
		323			−65.48	
		373			−75.49	
	C_3H_8	298	−5.44	0.19	−61.37	5.07
		323			−66.07	
		373			−75.45	
	C_2H_6	298	−5.29	0.19	−61.23	11.99
		323			−65.92	
		373			−75.30	
Hybrid Carbon membrane	CH_4	298	−20.60	0.14	−61.39	22.92
		323			−64.81	
		373			−71.66	
	C_3H_8	298	−13.49	0.16	−60.84	23.32
		323			−64.81	
		373			−72.75	
	C_2H_6	298	−15.87	0.15	−60.91	23.21
		323			−64.69	
		373			−72.25	

4.0 CONCLUSION

The current work was successfully produced a pristine carbon membrane and hybrid carbon membrane utilizing carbonization technique. XRD and SEM analyses were used to validate the material's structure. The obtained XRD pattern exhibited a distinctive graphitic phase. Furthermore, carbonization producing a reduction of the d-spacing number of membranes. Notably, the XRD findings agreed well with the SEM analysis, indicating the formation of dense and compact membrane structure. Gases permeabilities were investigated at three different operating temperatures (298, 323, and 373 K) in order to understand the gases' permeability characteristics. The highest CH_4/C_3H_8 (2.24) and CH_4/C_2H_6 (2.04) selectivity was observed on carbon membrane at 323 K due to higher C_3H_8 and C_2H_6 permeability decreasing as the contribution of higher ΔH value, while CH_4 permeability slightly increase because of the low ΔH value. The highest permeability of gases (CH_4, C_3H_8, and C_2H_6) was found on hybrid carbon membrane at 373K which contributed by the higher activation energies which represent the gas penetration tendency (22.92, 23.32, and 23.21 kJ mol^{-1}). The membrane transport mechanism involved adsorption and activated surface diffusion. The addition of filler in the carbon membrane creates more dependent permeation on temperature due to the contribution of the adsorption site of the ZCC with higher

surface area. Furthermore, the presence of ZCC improves thermal stability by slowing the membrane's decomposition rate.

CONFLICTS OF INTEREST

The authors declare that there is no conflict of interest regarding the publication of this paper.

ACKNOWLEDGEMENT

The authors like to express their gratitude for the research support granted by the PMDSU research grant from the Indonesian Ministry of Research and Higher Education, contract number: [028/SP2H/PTNBH/DRPM/2018]. Additionally, the authors would like to thank *Pertamina* and *Pembangunan Perumahan* Company for their financial support, as well as Shibaura Institute of Technology for granting a student exchange scholarship. Moreover, the authors gratefully acknowledge financial support from the Institut Teknologi Sepuluh Nopember for this work, under project scheme of the Publication Writing and IPR Incentive Programe (PPHKI) 2023.

REFERENCES

[1] A. Mohamed, S. Yousef, V. Makarevicius, A. Tonkonogovas. (2023). GNs/MOF-based mixed matrix membranes for gas separations. *Int. J. Hydrogen Energy, 48*, 19596-19604. https://doi.org/https://doi.org/10.1016/j.ijhydene.2023.02.074.

[2] A. K. Zulhairun, R. Wijiyanti, N. Widiastuti, P. S. Goh, A. F. Ismail. (2020). Prospects of nanocomposite membranes for natural gas treatment. In: *Nanocomposite Membr. Water Gas Sep*. Elsevier. 355-378. https://doi.org/10.1016/B978-0-12-816710-6.00014-6.

[3] G.- E. Alvarez. (2020). Optimization of the integration among traditional fossil fuels, clean energies, renewable sources, and energy storages: An MILP model for the coupled electric power, hydraulic, and natural gas systems. *Comput. Ind. Eng., 139*, 106141. https://doi.org/10.1016/j.cie.2019.106141.

[4] I. Tirouni, M. Sadeghi, M. Pakizeh. (2015). Separation of C3H8 and C2H6 from CH4 in polyurethane-zeolite 4Å and ZSM-5 mixed matrix membranes. *Sep. Purif. Technol., 141*, 394-402. https://doi.org/10.1016/j.seppur.2014.12.012.

[5] A. F. Ismail, K. Chandra Khulbe, T. Matsuura. (2015). *Gas Separation Membranes*. Springer International Publishing, Cham. https://doi.org/10.1007/978-3-319-01095-3.

[6] Z. Wu. (2019). Inorganic membranes for gas separations. In: *Membr. Sep. Princ. Appl.* Elsevier. 147-179. https://doi.org/10.1016/B978-0-12-812815-2.00005-3.

[7] S. Tanizume, S. Maehara, K. Ishii, T. Onoki, T. Okuno, H. Tawarayama, S. Ishikawa, M. Nomura. (2021). Reaction of methanol to olefin using a membrane contactor on a silica substrate. *Sep. Purif. Technol., 254*, 117647. https://doi.org/10.1016/j.seppur.2020.117647.

[8] S. Tanizume, T. Yoshimura, K. Ishii, M. Nomura. (2021).

Control of sequential mto reactions through an MFI-type zeolite membrane contactor. *Membranes (Basel). 10*, 117647. https://doi.org/10.3390/membranes10020026.

[9] Y. Sugiyama, S. Ikarugi, K. Oura, A. Ikeda, E. Matsuyama, R. Ono, M. Nomura, H. Tawarayama, T. Saito, K. Kuwahara. (2015). MFI zeolite membranes prepared on novel silica substrates. *J. Chem. Eng. Japan, 48*, 891-896. https://doi.org/10.1252/jcej.15we014.

[10] J. Yoshiura, K. Ishii, Y. Saito, T. Nagataki, Y. Nagataki, A. Ikeda, M. Nomura. (2020). Permeation properties of ions through inorganic silica-based membranes. *Membranes (Basel), 10*, 1-11. https://doi.org/10.3390/membranes10020027.

[11] K. Ishii, A. Shibata, T. Takeuchi, J. Yoshiura, T. Urabe, Y. Kameda, M. Nomura. (2019). Development of silica membranes to improve dehydration reactions. *J. Japan Pet. Inst., 62*, 211-219. https://doi.org/10.1627/jpi.62.211.

[12] W. H. Chen, C. W. Tsai, Y. L. Lin. (2017). Numerical studies of the influences of bypass on hydrogen separation in a multichannel Pd membrane system. *Renew. Energy, 104*, 259-270. https://doi.org/10.1016/j.renene.2016.12.032.

[13] E. P. Favvas, G. E. Romanos, F. K. Katsaros, K. L. Stefanopoulos, S. K. Papageorgiou, A. C. Mitropoulos, N. K. Kanellopoulos, K. Nick. (2016). Gas permeance properties of asymmetric carbon hollow fiber membranes at high feed pressures. *J. Nat. Gas Sci. Eng., 31*, 842-851. https://doi.org/10.1016/j.jngse.2016.03.089.

[14] M. Rungta, G. B. Wenz, C. Zhang, L. Xu, W. Qiu, J. S. Adams, W. J. Koros. (2017). Carbon molecular sieve structure development and membrane performance relationships. *Carbon N. Y., 115*, 237-248. https://doi.org/https://doi.org/10.1016/j.carbon.2017.01.015.

[15] J. B. S. Hamm, A. Ambrosi, J. G. Griebeler, N. R. Marcilio, I. C. Tessaro, L. D. Pollo. (2017). Recent advances in the development of supported carbon membranes for gas separation. *Int. J. Hydrogen Energy*, *42*, 24830-24845. https://doi.org/10.1016/j.ijhydene.2017.08.071.

[16] H. Li, K. Haas-santo, U. Schygulla, R. Dittmeyer. (2015). Inorganic microporous membranes for H_2 and CO_2 separation-Review of experimental and modeling progress. *127*, 401-417. https://doi.org/10.1016/j.ces.2015.01.022.

[17] O. Salinas, X. Ma, Y. Wang, Y. Han, I. Pinnau. (2017). Carbon molecular sieve membrane from a microporous spirobisindane-based polyimide precursor with enhanced ethylene/ethane mixed-gas selectivity. *RSC Adv., 7*, 3265-3272. https://doi.org/10.1039/c6ra24699k.

[18] R. Wijiyanti, A. R. Kumala Wardhani, R. A. Roslan, T. Gunawan, Z. Abdul Karim, A. F. Ismail, N. Widiastuti. (2020). Enhanced gas separation performance of polysulfone

membrane by incorporation of zeolite-templated carbon. *Malaysian J. Fundam. Appl. Sci., 16*, 128-134. https://doi.org/10.11113/mjfas.v16n2.1472.

[19] R. Wijiyanti, A. N. Ubaidillah, T. Gunawan, Z. A. Karim, A. F. Ismail, S. Smart, R. Lin, N. Widiastuti. (2019). Polysulfone mixed matrix hollow fiber membranes using zeolite templated carbon as a performance enhancement filler for gas separation. *Chem. Eng. Res. Des.*, *150*, 274-288. https://doi.org/10.1016/j.cherd.2019.08.004.

[20] I. S. Caralin, A. R. Widyanto, N. Widiastuti, R. Wijiyanti, T. Gunawan, Z. A. Karim, M. Nomura, Y. Yoshida. (2021). Annealing treatment for enhancing of H_2/C_3H_8 separation performance on polysulfone membrane. *AIP Conf. Proc., American Institute of Physics*, 020065. https://doi.org/10.1063/5.0052177.

[21] I. S. Caralin, A. R. Widyanto, N. Widiastuti, R. Wijiyanti, T. Gunawan, Z. A. Karim, M. Nomura, Y. Yoshida. (2022). Elevated H_2/N_2 separation performance by annealing post-treatment of polysulfone hollow fiber membrane. *Rasayan J. Chem.*, *15*, 2292-2298. https://doi.org/10.31788/RJC.2022.1546962.

[22] N. Widiastuti, I. S. Caralin, A. R. Widyanto, R. Wijiyanti, T. Gunawan, Z. A. Karim, M. Nomura, Y. Yoshida. (2022). Annealing and TMOS coating on PSF/ZTC mixed matrix membrane for enhanced CO_2/CH_4 and H_2/CH_4 separation. *R. Soc. Open Sci., 9*, 322-334. https://doi.org/10.1098/rsos.211371.

[23] R. Wijiyanti, I. S. Caralin, A. R. Widyanto, T. Gunawan, Z. A. Karim, A. F. Ismail, M. Nomura, N. Widiastuti. (2023). Evaluation of different carbon-modified zeolite derivatives preparation methods as a filler in mixed matrix membrane on their gas separation performance. *Microporous Mesoporous Mater*. *359*, 112650. https://doi.org/10.1016/j.micromeso.2023.112650.

[24] T. Gunawan, T. Q. Romadiansyah, R. Wijiyanti, W. N. Wan Salleh, N. Widiastuti. (2019). Zeolite templated carbon: Preparation, characterization and performance as filler material in co-polyimide membranes for CO_2/CH_4 separation. *Malaysian J. Fundam. Appl. Sci.*, *15*, 407-413. https://doi.org/10.11113/mjfas.v15n3.1461.

[25] P. Sari, T. Gunawan, W. N. Wan Salleh, A. F. Ismail, N. Widiastuti. (2019). Simple method to enhance O_2/N_2 separation on P84 co-polyimide hollow fiber membrane. *IOP Conf. Ser. Mater. Sci. Eng., 546*, 042042. https://doi.org/10.1088/1757-899X/546/4/042042.

[26] N. Widiastuti, T. Gunawan, H. Fansuri, W. N. W. Salleh, A. F. Ismail, N. Sazali. (2020). P84/ZCC hollow fiber mixed matrix membrane with PDMS coating to enhance air separation performance. *Membranes (Basel). 10*, 267. https://doi.org/10.3390/membranes10100267.

[27] T. Gunawan, N. Widiastuti, H. Fansuri, W. N. Wan Salleh, A. F. Ismail, R. Lin, J. Motuzas, S.

Smart. (2021). The utilization of micro-mesoporous carbon-based filler in the P84 hollow fibre membrane for gas separation. *R. Soc. Open Sci., 8*, https://doi.org/10.1098/rsos.201150.

[28] T. Gunawan, R. P. Rahayu, R. Wijiyanti, W. N. W. Salleh, N. Widiastuti. (2019). P84/zeolite-carbon composite mixed matrix membrane for CO_2/CH_4 separation, *Indones. J. Chem., 19*, 650-659. https://doi.org/10.22146/ijc.35727.

[29] A. R. Widyanto, I. S. Caralin, N. Widiastuti, T. Gunawan, R. Wijiyanti, W. N. W. Salleh, A. F. Ismail, M. Nomura, K. Suzuki. (2022). N_2/CH_4 separation behavior at elevated temperature on P84 hollow fiber carbon membrane. *Mater. Today Proc., 65*, 3093-3100. https://doi.org/10.1016/j.matpr.2022.05.533.

[30] X. Ma, R. Swaidan, B. Teng, H. Tan, O. Salinas, E. Litwiller, Y. Han, I. Pinnau. (2013). Carbon molecular sieve gas separation membranes based on an intrinsically microporous polyimide precursor. *Carbon N. Y., 62*, 88-96. https://doi.org/10.1016/j.carbon.2013.05.057.

[31] N. Widiastuti, A. R. Widyanto, I. S. Caralin, T. Gunawan, R. Wijiyanti, W. N. Wan Salleh, A. F. Ismail, M. Nomura, K. Suzuki. (2021). Development of a P84/ZCC Composite Carbon Membrane for Gas Separation of H_2/CO_2 and H_2/CH_4. *ACS Omega, 6*, 15637-15650. https://doi.org/10.1021/acsomega.1c00512.

[32] A. R. Widyanto, I. S. Caralin, N. Widiastuti, T. Gunawan, R. Wijiyanti, W. N. W. Salleh, A. F. Ismail, M. Nomura, K. Suzuki. (2021). Improvement N_2/SF_6 separation performance on P84 derived carbon membrane by incorporating of zeolite-carbon composite. *AIP Conf. Proc., American Institute of Physics*. 020008. https://doi.org/10.1063/5.0052171.

[33] F. H. Saboor, O. Hajizadeh. (2020). Separation of light hydrocarbons: A minireview. *Adv. J. Chem. A.*, *2020*, 777-788. https://doi.org/10.22034/AJCA.2020.114713.

[34] K. A. Stevens, J. D. Moon, H. Borjigin, R. Liu, R. M. Joseph, J. S. Riffle, B. D. Freeman. (2020). Influence of temperature on gas transport properties of tetraaminodiphenylsulfone (TADPS) based polybenzimidazoles. *J. Memb. Sci., 593.* https://doi.org/10.1016/j.memsci.2019.117427.

[35] S. Fu, E. S. Sanders, S. S. Kulkarni, G. B. Wenz, W. J. Koros. (2015). Temperature dependence of gas transport and sorption in carbon molecular sieve membranes derived from four 6FDA based polyimides: Entropic selectivity evaluation. *Carbon N. Y., 95*, 995-1006. https://doi.org/10.1016/j.carbon.2015.09.005.

[36] S. Fu, E. S. Sanders, S. Kulkarni, Y. H. Chu, G. B. Wenz, W. J. Koros. (2017). The significance of entropic selectivity in carbon molecular sieve membranes derived from 6FDA/DETDA:DABA(3:2) polyimide. *J. Memb. Sci.*, *539,* 329-343. https://doi.org/10.1016/j.memsci.2017.06.007.

[37] M. Yoshimune, I. Fujiwara, K. Haraya. (2007). Carbon molecular sieve membranes derived from trimethylsilyl substituted poly (phenylene oxide) for gas separation. *Carbon*, *45*, 553-560. https://doi.org/10.1016/j.carbon.2006.10.017.

[38] Y. K. Kim, H. B. Park, Y. M. Lee. (2005). Gas separation properties of carbon molecular sieve membranes derived from polyimide/polyvinylpyrrolidone blends: Effect of the molecular weight of polyvinylpyrrolidone. *J. Memb. Sci., 251*, 159-167. https://doi.org/10.1016/j.memsci.2004.11.011.

[39] R. Wijiyanti, T. Gunawan, N. S. Nasri, Z. A. Karim, A. F. Ismail, N. Widiastuti. (2019). Hydrogen adsorption characteristics for zeolite-Y templated carbon. *Indones. J. Chem., 20*, 29. https://doi.org/10.22146/ijc.38978.

[40] T. Gunawan, R. Wijiyanti, N. Widiastuti. (2018). Adsorption–desorption of CO_2 on zeolite-Y-templated carbon at various temperatures. *RSC Adv., 8*, 41594-41602. https://doi.org/10.1039/C8RA09200A.

[41] Z. Yang, H. Peng, W. Wang, T. Liu. (2010). Crystallization behavior of poly(ε-caprolactone)/layered double hydroxide nanocomposites. *J. Appl. Polym. Sci.*, *116*, 2658-2667. https://doi.org/10.1002/app.

[42] Y. Wang, J. E. Panzik, B. Kiefer, K. K. M. Lee. (2012). Crystal structure of graphite under room-temperature compression and decompression. *Sci. Rep., 2*, 520. https://doi.org/10.1038/srep00520.

[43] L. Olivieri, A. Tena, M. G. De Angelis, A. Hernández Giménez, A. E. Lozano, G. C. Sarti. (2016). The effect of humidity on the CO_2/N_2 separation performance of copolymers based on hard polyimide segments and soft polyether chains: Experimental and modeling. *Green Energy Environ., 1*, 201-210. https://doi.org/10.1016/j.gee.2016.09.002.

[44] N. Sazali, W. N. W. Salleh, A. F. Ismail, N. H. Ismail, M. A. Mohamed, N. A. H. M. Nordin, M. N. M. M. Sokri, Y. Iwamoto, S. Honda. (2018). Enhanced gas separation performance using carbon membranes containing nanocrystalline cellulose and BTDA-TDI/MDI polyimide. *Chem. Eng. Res. Des., 140*, 221-228. https://doi.org/10.1016/j.cherd.2018.09.039.

[45] X. He, M.-B. B. Hägg. (2012). Structural, kinetic and performance characterization of hollow fiber carbon membranes, *J. Memb. Sci.,* 390-39123-31. https://doi.org/10.1016/j.memsci.2011.10.052.

[46] P. S. Tin, T. S. Chung, Y. Liu, R. Wang. (2004). Separation of CO_2/CH_4 through carbon molecular sieve membranes derived from P84 polyimide. *Carbon N. Y., 42*, 3123-3131. https://doi.org/10.1016/j.carbon.2004.07.026.

[47] N. Widiastuti, T. Gunawan, H. Fansuri, W. N. W. Salleh, A. F. Ismail, N. Sazali. (2020). P84/ZCC hollow fiber mixed matrix membrane with PDMS coating to enhance air separation performance. *Membranes (Basel)., 10*, 267. https://doi.org/10.3390/membran

es10100267.

[48] M. Kiyono, P. J. Williams, W. J. Koros. (2010). Effect of pyrolysis atmosphere on separation performance of carbon molecular sieve membranes. *J. Memb. Sci., 359*, 2-10. https://doi.org/10.1016/j.memsci.2009.10.019.

[49] J. Gilron, A. Soffer. (2002). Knudsen diffusion in microporous carbon membranes with molecular sieving character. *J. Memb. Sci., 209*, 339-352. https://doi.org/https://doi.org/10.1016/S0376-7388(02)00074-1.

[50] F. J. Sotomayor, K. A. Cychosz, M. Thommes, F. Sotomayor, K. A. Cychosz, M. Thommes. (2018). Characterization of Micro/mesoporous materials by physisorption : Concepts and case studies. *Accounts Mater. Surf. Res., 3*, 34-50.

[51] N. H. Ismail, W. N. W. Salleh, N. Sazali, A. F. Ismail. (2018). Development and characterization of disk supported carbon membrane prepared by one-step coating-carbonization cycle. *J. Ind. Eng. Chem., 57*, 313-321. https://doi.org/10.1016/j.jiec.2017.08.038.

[52] S. S. Hosseini, T. S. Chung. (2009). Carbon membranes from blends of PBI and polyimides for N_2/CH_4 and CO_2/CH_4 separation and hydrogen purification. *J. Memb. Sci., 328*, 174-185. https://doi.org/10.1016/j.memsci.2008.12.005.

[53] Y. Wu, J. Zhou, B. Zhang, D. Zhao, L. Li, Y. Lu, T. Wang. (2016). Fabrication and gas permeation of CMS/C composite membranes based on polyimide and phenolic resin. *RSC Adv., 6*, 75390-75399. https://doi.org/10.1039/C6RA12476C.

[54] E. P. Favvas, G. E. Romanos, S. K. Papageorgiou, F. K. Katsaros, A. C. Mitropoulos, N. K. Kanellopoulos. (2011). A methodology for the morphological and physicochemical characterisation of asymmetric carbon hollow fiber membranes. *J. Memb. Sci., 375*, 113-123. https://doi.org/10.1016/j.memsci.2011.03.028.

[55] L. T. Y. Au, W. Yin Mui, P. Sze Lau, C. Tellez Ariso, K. L. Yeung. (2001). Engineering the shape of zeolite crystal grain in MFI membranes and their effects on the gas permeation properties. *Microporous Mesoporous Mater., 47*, 203-216. https://doi.org/10.1016/S1387-1811(01)00380-8.

[56] M. P. Bernal, J. Coronas, M. Menéndez, J. Santamaría. (2002). Characterization of zeolite membranes by temperature programmed permeation and step desorption. *J. Memb. Sci., 195*, 125-138. https://doi.org/10.1016/S0376-7388(01)00557-9.

[57] Z. Lai, M. Tsapatsis. (2004). Gas and organic vapor permeation through b-oriented MFI membranes. *Ind. Eng. Chem. Res., 43*, 3000-3007. https://doi.org/10.1021/ie034096s.

[58] J. C. Poshusta, R. D. Noble, J. L. Falconer. (1999). Temperature and pressure effects on CO_2 and CH_4 permeation through MFI zeolite membranes. *J. Memb. Sci., 160*, 115-125. https://doi.org/10.1016/S0376-7388(99)00073-3.

[59] G. G. Kagramanov, I. P. Storojuk, E. N. Farnosova.

(2016). Vapour and acid components separation from gases by membranes principles and engineering approach to membranes development. *J. Phys. Conf. Ser., 751*, https://doi.org/10.1088/1742-6596/751/1/012039.

[60] A. Khosravi, M. Sadeghi, H. Z. Banadkohi, M. M. Talakesh. (2014). Polyurethane-silica nanocomposite membranes for separation of propane/methane and ethane/methane. *Ind. Eng. Chem. Res., 53*, 2011-2021. https://doi.org/10.1021/ie403322w.

[61] Q. Wang, F. Huang, C. J. Cornelius, Y. Fan. (2021). Carbon molecular sieve membranes derived from crosslinkable polyimides for CO_2/CH_4 and C_2H_4/C_2H_6 separations. *J. Memb. Sci., 621*, 118785. https://doi.org/10.1016/j.memsci.2020.118785.

[62] L. Xu, M. Rungta, M. K. Brayden, M. V. Martinez, B. A. Stears, G. A. Barbay, W. J. Koros. (2012). Olefins-selective asymmetric carbon molecular sieve hollow fiber membranes for hybrid membrane-distillation processes for olefin/paraffin separations. *J. Memb. Sci.,* 423-424, 314-323. https://doi.org/10.1016/j.memsci.2012.08.028.

[63] K. M. Steel, W. J. Koros. (2005). An investigation of the effects of pyrolysis parameters on gas separation properties of carbon materials. *Carbon N. Y.,* 43, 1843-1856. https://doi.org/10.1016/j.carbon.2005.02.028.

[64] R. L. Tseng, F. C. Wu, R. S. Juang. (2015). Adsorption of CO_2 at atmospheric pressure on activated carbons prepared from melamine-modified phenol-formaldehyde resins. *Sep. Purif. Technol., 140*, 53-60. https://doi.org/10.1016/j.seppur.2014.11.018.

[65] D. Tondeur, E. Kvaalen. (1987). Equipartition of entropy production. An optimality criterion for transfer and separation processes. *Ind. Eng. Chem. Res., 26*, 50-56. https://doi.org/10.1021/ie00061a010.